Electrochemical investigation of corrosion and corrosion inhibition of copper in NaCl solutions

N. A. Al-Mobarak [a], K. F. Khaled [b,c], O.A. Elhabib [c], K. M. Abdel-Azim [b]

[a]*Faculty of Science, Girls Section, Chemistry Department, Princess Nora bint Abdulrahman University, Riyadh, Kingdom of Saudi Arabia*
[b]*Electrochemistry Research Laboratory, Chemistry Department, Faculty of Education, Ain Shams University, Roxy, Cairo, Egypt*
[c]*Materials and Corrosion Laboratory, Chemistry Department, Faculty of Science ,Taif University,Taif, Hawiya 888, Kingdom of Saudi Arabia*

* *Corresponding author. E-mail:* khaledrice2003@yahoo.com

Received: 5 May 2010; revised version 13 June 2010; accepted: 20 June 2010

Abstract

Inhibition effect of a new pyrimidine heterocyclic derivative, namely 2-hydrazino-4-(p-methoxyphenyl)-6-oxo-1,6-dihydropyrimidine-5-carbonitrile (HPD) on copper corrosion in 3.5% NaCl solutions at 25°C ±1 was investigated by using potentiodynamic polarization , electrochemical impedance spectroscopy, EIS and electrochemical frequency modulation, EFM. The electrochemical measurements demonstrated that, under the chosen experimental conditions HPD offers sufficient inhibition against copper corrosion in 3.5% NaCl solutions. Tafel polarization studies have shown that the HPD suppresses both the cathodic and anodic processes and thus it acts as mixed-type inhibitor. The results of EIS indicate that the value of CPEs tends to decrease and both charge transfer resistance and inhibition efficiency tend to increase by increasing the inhibitor concentration. EFM can be used as a rapid and non destructive technique for corrosion rate measurements without prior knowledge of Tafel constants. Molecular dynamic simulations are performed to investigate the adsorption behaviour of HPD on copper surface.

Keywords: Copper; EFM, Corrosion inhibition, Molecular dynamics

1. Introduction

Copper has been one of more important materials in industry owing to its high electrical and thermal conductivities, mechanical workability and its relatively noble properties. It is widely used in many applications in electronic industries and communications as a conductor in electrical power lines, pipelines for domestic and industrial water utilities including sea water, heat conductors, heat exchangers, etc. Therefore, corrosion of copper and its inhibition in a wide variety of media, particularly when they contain chloride ions, have attracted the attention of many investigators [1-11].

The corrosion of copper and its alloys depends to a great extent on the makeup of the electrolyte in contact with the metal surface. The mechanism involves copper dissolution at local anodic sites and electrochemical reduction of some species such as oxygen at cathodic areas. A given surface area may alternate from being anode and cathode to produce uniform corrosion. In chloride solutions, the first step of the anodic dissolution is the formation of $CuCl_2^-$ complex. In addition, it was found that during anodic polarization, there is always equilibrium between a thin layer of $CuCl$ and a dense layer of dissolved $CuCl_2^-$ [12]. In natural fresh water, protecting coatings, such as Cu_2O and $Cu(OH)_2$ are formed on copper. These layers are important in different regards; they are useful for their corrosion protection properties and they influence electrochemical processes at copper electrodes [13-15].

The role of Cl^- ions in copper corrosion in NaCl centered around (i) a competitive adsorption with OH^- on the available Cu surface, thus creating sites that are more liable for electrochemical dissolution, and (ii) competition with OH^- attached to Cu(II) ions in a soluble intermediate stage, thus enhancing film rupture through dissolution [16].
The inhibition action of certain organic compounds on metallic corrosion processes has been extensively studied in recent years [17-22]. The exact nature of the interaction between the inhibitors and the metallic surface is, however, far from being explained and general conclusions are more difficult to draw. There is agreement of some stages participating in the overall inhibition process, particularly with respect to the mechanism in which inhibition occurs.
Heterocyclic organic compounds have generally been used as corrosion inhibitors due to their high inhibition efficiency. The present work aims to characterize the effect of a new heterocyclic pyrimidine derivative as corrosion inhibitor for Cu in 3.5% NaCl solution using electrochemical methods. It is also, the aim of this study to investigate the interaction between the pyrimidine derivative and the copper surface in 3.5% NaCl using molecular dynamics simulations.

2. Experimental

In this study a new pyrimidine heterocyclic derivative, namely 2-hydrazino-4-(p-methoxyphenyl)-6-oxo-1,6-dihydropyrimidine-5-carbonitrile (HPD) was prepared in our laboratory where a mixture of 2-ethylthio-4-(p-methoxyphenyl)-6-oxo-1,6-dihydropyrim-idine-5-carbonitrile (0.01 mole) and hydrazine hydrate (15 ml) were heated under reflux for 6 h. The reaction mixture was cooled and poured gradually onto crushed ice. The solid obtained was filtered off and re-crystallized from DMF to give HPD as pale yellow crystals, yield 85%, m.p. 235 ºC, its structure was confirmed with different spectroscopic techniques [24] and presented below:

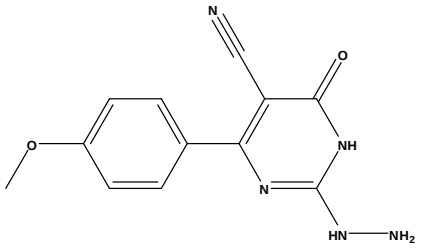

Scheme: Molecular structure of 2-hydrazino-4-(p-methoxyphenyl)-6-oxo-1,6-dihydropyrimidine-5-carbonitrile (HPD)

The HPD is added to the 3.5% NaCl at concentrations of 5×10^{-5}, 10^{-4}, 5×10^{-4} and 10^{-3} M.

Cylindrical rods of copper specimens obtained from Johnson Mattey (Puratronic, 99.999%) were mounted in Teflon. An epoxy resin was used to fill the space between Teflon and Cu electrode. The circular cross sectional area of the copper rod exposed to the corrosive medium, used in electrochemical measurements, was (0.28 cm^2).

The electrochemical measurements were performed in a typical three-compartment glass cell consisted of the copper specimen as working electrode (WE), platinum counter electrode (CE), and a saturated calomel electrode (SCE) as the reference electrode. The counter electrode was separated from the working electrode compartment by fritted glass. The reference electrode was connected to a Luggin capillary to minimize IR drop. Solutions were prepared from bidistilled water of resistivity 13 MΩ cm, the copper electrode was abraded with different grit emery papers up to 4/0 grit size, cleaned with acetone, washed with bidistilled water and finally dried.

Tafel polarization curves were obtained by changing the electrode potential automatically from (-750 to + 300 mV_{SCE}) at open circuit potential with scan rate of 1.0 mV s^{-1}. Impedance measurements were carried out in frequency range from 100 kHz to 40 mHz with an amplitude of 10 mV peak-to-peak using ac signals at open circuit potential. Electrochemical frequency modulation, EFM, was carried out using two frequencies 2 Hz and 5 Hz. The base frequency was 1 Hz, so the waveform repeats after 1 second. The higher frequency must be at least two times the lower one. The higher frequency must also be sufficiently slow that the charging of the double layer does not contribute to the current response. Often, 10 Hz is a reasonable limit.

The electrode potential was allowed to stabilize 60 min before starting the measurements. All experiments were conducted at 25 ± 1 °C. Measurements were performed using Gamry Instrument Potentiostat/Galvanostat/ZRA.

This includes a Gamry Framework system based on the ESA400, Gamry applications that include dc105 for dc corrosion measurements, EIS300 for electrochemical impedance spectroscopy and EFM 140 for electrochemical frequency modulation measurements along with a computer for collecting data. Echem Analyst 5.58 software was used for plotting, graphing and fitting data.

3. Computational details

The geometry optimization process is carried out for the studied HPD compound using an iterative process, in which the atomic coordinates are adjusted until the total energy of a structure is minimized, i.e., it corresponds to a local minimum in the potential energy surface. The forces on the atoms in the HPD molecules are calculated from the potential energy expression and will, therefore, depend on the force field that is selected.

Interaction between HPD and Cu (111) surface was carried out in a simulation box (16.45 Å × 16.45 Å × 40.15 Å) with periodic boundary conditions to model a representative part of the interface devoid of any arbitrary boundary effects. The Cu (111) was first built and relaxed by minimizing its energy using molecular mechanics, then the surface area of Cu (111) was increased and its periodicity is changed by constructing a super cell, and then a vacuum slab with 30 Å thicknesses was built on the Cu (111) surface. The number of layers in the structure was chosen so that the depth of the surface is greater than the non-bond cutoff used in calculation. Using 6 layers of Cu atoms gives a sufficient depth that the inhibitor molecules will only be involved in non-bond interactions with Cu atoms in the layers of the surface, without increasing the calculation time unreasonably. This structure then converted to have 3D periodicity. As 3D periodic boundary conditions are used, it is important that the size of the vacuum slab is great enough (30 Å) that the non-bond calculations for the adsorbate (HPD molecules) does not interact with the periodic image of the bottom layer of atoms in the surface. After minimizing the Cu (111) surface and HPD molecules, the corrosion system will be built by layer builder to place the inhibitor molecules on Cu (111) surface, and the behaviours of the HPD molecules on the Cu (111) surface were simulated using the COMPASS (condensed phase optimized molecular potentials for atomistic simulation studies) force field.

The Discover molecular dynamics module in Materials Studio 5.0 software from Accelrys Inc. [25] allows selecting a thermodynamic ensemble and the associated parameters, defining simulation time, temperature and pressuring and initiating a dynamics calculation. The molecular dynamics simulations procedures have been described elsewhere [26]. The interaction energy, $E_{Cu\text{-}inhibitor}$, of the Cu (111) surface with HPD was calculated according to the following equation:

$$E_{Cu\text{-}inhibitor} = E_{complex} - (E_{Cu\text{-}surface} + E_{inhibitor}) \quad (1)$$

where $E_{complex}$ is the total energy of the Cu (111) surface together with the adsorbed inhibitor molecule, $E_{Cu\text{-}surface}$ and $E_{inhibitor}$ are the total energy of the Cu (111) surface and free inhibitor molecule, respectively. The binding energy between HPD and Cu (111) surfaces, was the negative value of the interaction energy [27], as follow:

$$E_{binding} = -E_{Cu\text{-}inhibitor} \quad (2)$$

4. Results and discussion

4.1 Potentiodynamic polarization measurements

When a copper specimen is immersed in 3.5% NaCl, both reduction and oxidation processes occur on its surface. Typically, the copper specimen oxidizes (corrodes) and the oxygen is reduced. The cathodic reaction of copper in aerated sodium chloride solutions is well known to be the oxygen reduction [1,28]:

$$O_2 + 2H_2O + 4e^- \rightarrow 4OH^- \quad (3)$$

Any corrosion processes that occur are usually a result of anodic currents. When a copper specimen is in contact with a corrosive liquid and the specimen is not connected to any instrumentation as it would be "in service" the specimen assumes a potential (relative to a reference electrode) termed the corrosion potential, E_{corr}.The corrosion

potential, E_{corr} can be defined as the potential at which the rate of oxidation is exactly equal to the rate of reduction [29].

The potentiodynamic polarization curves recorded for the copper electrode in the absence and presence of HPD are presented in Fig. 1. It is obvious from Fig. 1 that the anodic branch of Cu in both NaCl solutions in the absence and the presence of HPD molecules shows a three distinct regions; firstly increasing the current from the Tafel region at lower over-potentials, which extending to the peak current density due to the dissolution of copper metal to Cu^+.

$$Cu \rightarrow Cu^+ + e^- \quad (4)$$

Secondly, the region of decreasing currents until a minimum is reached due to the formation of $CuCl$

$$Cu^+ + Cl^- \rightarrow CuCl \quad (5)$$

And finally the region of sudden increase in current density leading to a limiting value as a result of $CuCl_2^-$ formation which is the responsible on the dissolution of Cu

$$CuCl + Cl^- \rightarrow CuCl_2^- \quad (6)$$

It is also seen that increasing the HPD concentrations, decreases the cathodic, anodic and corrosion currents (i_{corr}) and consequently the corrosion rates.

It has been shown that in the Tafel extrapolation method, the use of both the anodic and cathodic Tafel regions is undoubtedly preferred over the use of only one Tafel region [30]. However, the corrosion rate can also be determined by Tafel extrapolation of either the cathodic or anodic polarization curve alone. If only one polarization curve is used, it is generally the cathodic curve which usually produces a longer and better defined Tafel region. Anodic polarization may sometimes produce concentration effects, due to passivation and dissolution, as well as roughening of the surface which can lead to deviations from Tafel behaviour.

Table 1 Electrochemical kinetic parameters obtained by potentiodynamic technique for copper in 3.5% NaCl without and with various concentrations of HPD at 25°C±1.

HPD / M	i_{corr} / μA cm^{-2}	$-E_{corr}$ / mV (SCE)	β_a / mV dec^{-1}	E_p(%)
Blank	11.30	293	227.0	-
5×10^{-5}	5.53	311	185.5	80.46
10^{-4}	4.93	282	189.5	82.58
5×10^{-4}	3.97	304	196.5	85.97
10^{-3}	2.93	264	189.1	89.65

The situation is quite different here; the anodic dissolution of copper in aerated 3.5% NaCl solutions obeys, as previously mentioned, Tafel's law. The anodic curve is, therefore preferred over the cathodic one for evaluation of corrosion currents, i_{corr}, by the Tafel extrapolation method. However, the cathodic polarization curve deviate from the Tafel behaviour, exhibiting a limiting diffusion current, may be due to the reduction of dissolved oxygen. Accordingly, there is an uncertainty and source of error in the numerical values of the cathodic Tafel slopes calculated by the Echem Analyst software. This is the reason why values of the cathodic Tafel slopes are not included here.

Addition of 10^{-3} M of HPD reduces to a great extent the cathodic and anodic currents, i_{corr}. The corresponding electrochemical kinetics parameters such as corrosion potential (E_{corr}), anodic Tafel slopes (β_a) and corrosion current density (i_{corr}), obtained by extrapolation of the Tafel lines are presented in Table 1. The inhibitor efficiency was evaluated from dc measurements using the following equation [31]:

$$E_p\% = \left(1 - \frac{i_{corr}}{i_{corr}^o}\right) \times 100 \quad (7)$$

where i_{corr}^o and i_{corr} correspond to uninhibited and inhibited current densities, respectively.

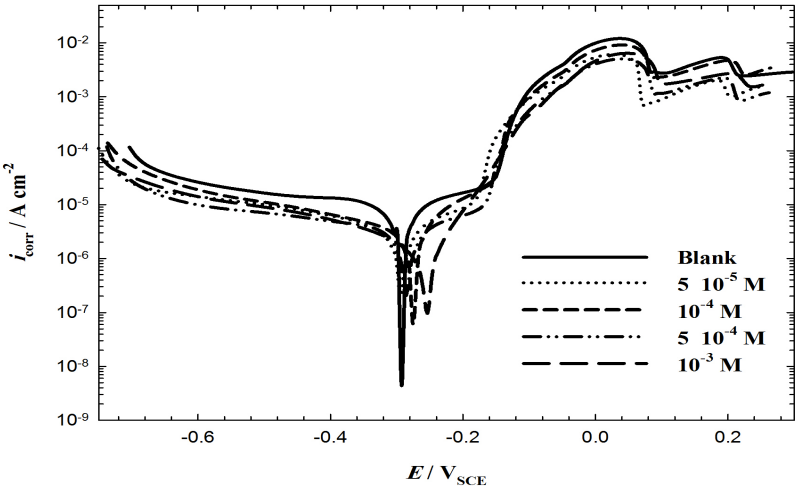

Figure 1. Anodic and cathodic polarization curves for copper in 3.5% NaCl solutions in the absence and presence of various concentrations of HPD at 25 °C±1.

Table 2 Electrochemical parameters calculated from EIS measurements on copper electrode in 3.5% NaCl solutions without and with various concentrations of HPD derivatives 25±1 °C using equivalent circuit presented in Fig. 3.

HPD/ M	R_s / Ω cm^2	R_p / Ω cm^2	CPE$_1$ $\mu\Omega^{-1}$cm^{-2}S^{n_1}	n_1	R_p'/ Ω cm^2	CPE$_2$ $\mu\Omega^{-1}$cm^{-2}S^{n_2}	n_2	W $\mu\Omega^{-1}$cm^{-2}S$^{1/2}$	η%
Blank	113	733	1.3	0.89	6.1	13.5	0.52	20.3	-
5 × 10^{-5}	91.3	3751	0.78	0.83	10.8	7.9	0.48	14.5	82.1
10^{-4}	90.2	4207	0.56	0.79	12.4	5.7	0.49	8.9	83.5
5 × 10^{-4}	87.6	5224	0.48	0.91	13.5	5.1	0.60	5.6	86.4
10^{-3}	90.7	7082	0.41	0.79	17.9	3.4	0.54	3.2	91.3

Inspection of Fig. 1 and Table 1 show the variation of E_{corr} values with the concentration of HPD in 3.5% NaCl solutions. As it can be seen, the corrosion potential (E_{corr}) have no definite shift and (i_{corr}) decreases when the concentration of HPD is increased. Absence of significant change in the anodic Tafel slope (β_a) in the presence of HPD indicates that the corrosion mechanism is not changed after adding the HPD.
HPD is thus a mixed-type inhibitor, meaning that the addition of HPD to 3.5% NaCl solutions reduces the anodic dissolution of copper, corresponding to a noticeable decrease in the current densities of the passivation plateau, and also retards the cathodic reactions that occurs on the copper surface.

4.2. Impedance measurements

Impedance spectra for copper in 3.5% NaCl solutions, without and with different concentrations of HPD, were similar in shape. The shape of the impedance diagrams of copper in 3.5% NaCl is similar to those found in the literature [32]. The presence of HPD increases the impedance but does not change the other aspects of corrosion mechanism occurred due to its addition. Fig. 2 shows the Nyquist plots for copper in 3.5% NaCl without and with different concentrations of HPD. Symbols represent the measured data and solid lines represent the fitting data obtained using the equivalent circuit [33] presented in Fig. 3. The parameters obtained by fitting the experimental data using the equivalent circuit (Fig. 3), and the calculated inhibition efficiencies are listed in Table 2, where R_s represents the solution resistance, R_p is the polarization resistance and can be defined also as the charge-transfer resistance, CPE$_1$ and CPE$_2$ are constant phase elements (CPEs), R_p' is another polarization resistance and W, is the Warburg impedance. The Nyquist plots presented in Fig. 2 clearly demonstrate that the shapes of these plots for inhibited copper electrode are not substantially different from those of uninhibited electrode. Addition of HPD molecules increases the impedance but does not change the other aspects of the electrode behaviour. Nyquist spectra presented in Fig. 2 are modeled using an equivalent circuit model similar to the one proposed by several authors [34,35].

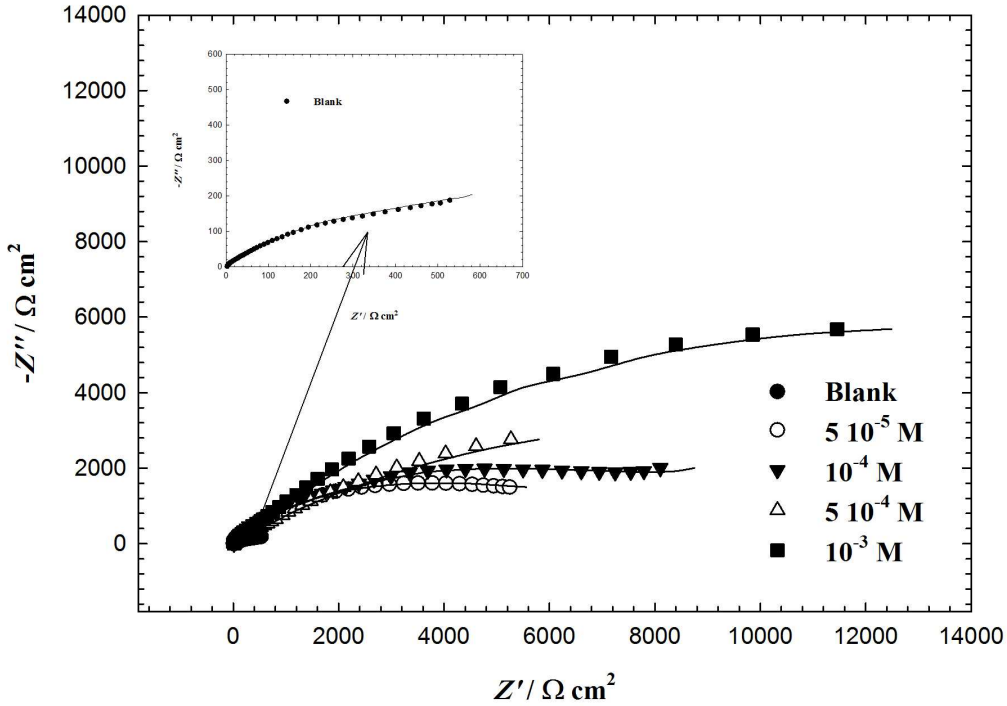

Figure 2 Nyquist plots for copper in 3.5% NaCl solutions in the absence and presence of various concentrations of HPD at 25 °C±1.

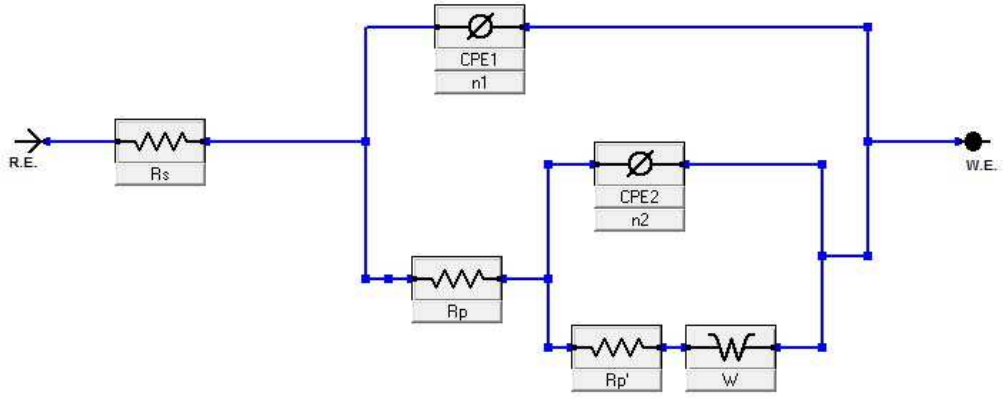

Figure 3 Equivalent circuits used to model impedance data for copper in 3.5% NaCl solutions in the absence and presence of various concentrations of HPD at 25 °C±1

The impedance spectra obtained for copper in 3.5% NaCl contains depressed semicircle with the center under the real axis, such behaviour is characteristic for solid electrodes and often referred to as frequency dispersion and attributed to the roughness and other inhomogenities of the solid electrode [36,37].

Parameters derived from EIS measurements and inhibition efficiency is given in Table 2. Addition of HPD increases the values of R_p and $R_p^{'}$ and lowers the values of CPE_1 and CPE_2 and this effect is seen to be increased as the concentrations of HPD increase. The constant phase elements (CPEs) with their n values $1 > n > 0$ represent double layer capacitors with some pores [33]. The CPEs decrease upon increase in HPD concentrations, which are expected to cover the charged surfaces and reducing the capacitive effects.

This decrease in (CPE) results from a decrease in local dielectric constant and/or an increase in the thickness of the double layer, suggested that HPD molecules inhibit the copper corrosion by adsorption at the copper/NaCl interface The semicircles at high frequencies in Fig. 2 are generally associated with the relaxation of electrical double layer capacitors and the diameters of the high frequency semicircles can be considered as the charge-transfer resistance ($R_{ct} = R_p$) [36]. Therefore, the inhibition efficiency, η% of HPD for the copper electrode can be calculated from the charge-transfer resistance as follows [36]:

$$\eta\% = (1-\frac{R_p^o}{R_p})\times 100 \quad (8)$$

where R_p^o and R_p are the polarization resistances for uninhibited and inhibited solutions, respectively. The CPEs are almost like Warburg impedance with their *n* values close to 0.5 in presence of HPD [33], which suggests that the electron transfer reaction corresponding to the second semicircle takes place through the surface layer and limits the mass transport (Warburg). The presence of the Warburg (*W*) impedance in the circuit confirms also that the mass transport is limited by the surface passive film.

4.3. Electrochemical frequency modulation, EFM

The EFM intermodulation spectra (spectra of current response as a function of frequency) were constructed for copper in aerated stagnant 3.5 M NaCl solutions without and with various concentrations of the tested inhibitors at 25 ± 1 °C; typical data are depicted in Fig. 4.

Corrosion kinetic parameters listed in Table 3 are calculated from EFM measurements using the following equations [38,39]:

$$i_{corr} = \frac{i_\omega^{\,2}}{\sqrt{48\left(2i_\omega i_{3\omega} - i_{2\omega}\right)}} \quad (9)$$

$$\beta_a = \frac{i_\omega U_o}{2i_{2\omega} + 2\sqrt{3}\sqrt{2i_{3\omega}i_\omega - i_{2\omega}^2}} \quad (10)$$

$$\beta_c = \frac{i_\omega U_o}{2\sqrt{3}\sqrt{2i_{3\omega}i_\omega - i_{2\omega}^2 - 2i_{2\omega}}} \quad (11)$$

$$\text{Causality factor (2)} = \frac{i_{\omega_2 \pm \omega_1}}{i_{2\omega_1}} = 2.0 \quad (12)$$

$$\text{Causality factor (3)} = \frac{i_{2\omega_2 \pm \omega_1}}{i_{3\omega_1}} = 3.0 \quad (13)$$

where *i* is the instantaneous current density at the working copper electrode measured at frequency ω and U_o is the amplitude of the sine wave distortion

Table 3 shows the corrosion kinetic parameters such as inhibition efficiency (E_{EFM} %), corrosion current density (μA/cm^2), Tafel constants (β_a , β_c) and causality factors (CF-2, CF-3) at different concentration of HPD derivatives in 3.5% NaCl at 25 ± 1 °C.

It is obvious from Table 3 that, the corrosion current densities decrease by increasing the concentrations of these compounds. The inhibition efficiencies increase by increasing HPD concentrations. The causality factors in Table 3 are very close to theoretical values which according to the EFM theory [38] should guarantee the validity of Tafel slopes and corrosion current densities. Inhibition efficiency (E_{EFM}%) depicted in Table 3 calculated from the following equation:

$$E_{EFM}\% = (1-\frac{i_{corr}}{i_{corr}^o}) \times 100 \quad (14)$$

where i_{corr}^o and i_{corr} are corrosion current density in the absence and the presence of HPD compound, respectively.

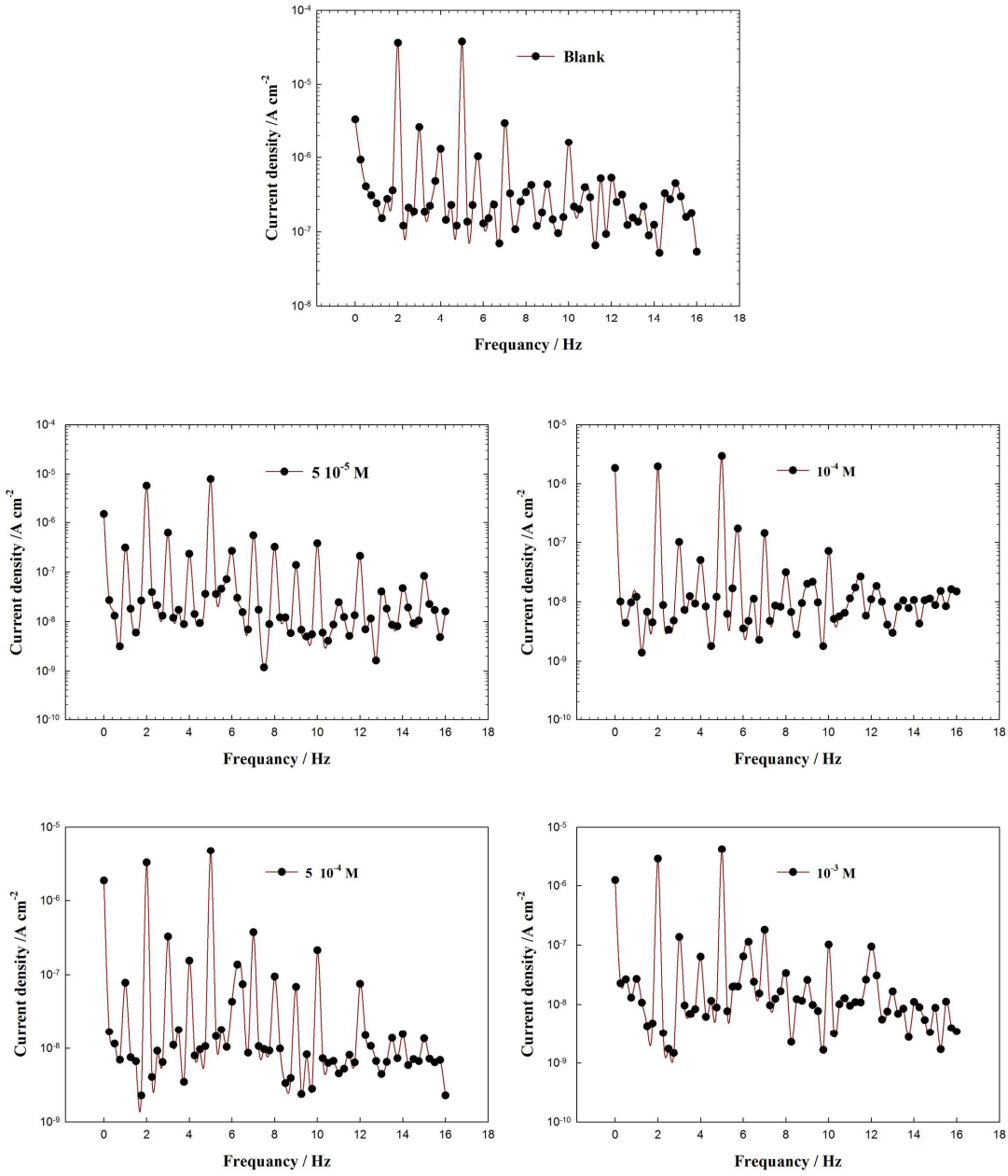

Figure 4 Intermodulation spectra recorded for copper electrode in 3.5% NaCl solutions in the absence and presence of various concentrations of HPD at 25 °C±1.

As can be seen from Table 3, the corrosion current densities decrease with increase in HPD concentrations. The causality factors in Table 3 indicate that the measured data are of good quality. The standard values for CF-2 and CF-3 are 2.0 and 3.0, respectively. The causality factor is calculated from the frequency spectrum of the current response. If the causality factors differ significantly from the theoretical values of 2.0 and 3.0, then it can be deduced that the measurements are influenced by noise. If the causality factors are approximately equal to the predicted values of 2.0 and 3.0, there is a causal relationship between the perturbation signal and the response signal. Then the data are assumed to be reliable [39]. When CF-2 and CF-3 are in the range 0–2 and 0–3, respectively, then the EFM data is valid.

The great strength of the EFM is the causality factors which serve as an internal check on the validity of the EFM measurement [39-40] . With the causality factors the experimental EFM data can be verified. The standard values for CF-2 and CF-3 are 2.0 and 3.0, respectively.

Table 3 Electrochemical kinetic parameters obtained by EFM technique for copper in 3.5% NaCl with various concentrations of PMD at 25°C.

HPD / M	i_{corr} / μA cm^{-2}	β_a / mV dec^{-1}	β_c / mV dec^{-1}	C.R /mpy	E_{EFM} %	CF-2	CF-3
Blank	71.75	71.76	119.1	117.1	-	1.9	1.4
5×10^{-5}	8.58	54.15	75.70	13.89	88.04	1.95	2.51
10^{-4}	7.45	71.25	115.20	12.88	89.62	1.86	2.45
5×10^{-4}	5.78	116.35	179.90	10.56	91.94	1.97	2.96
10^{-3}	4.25	91.65	122.70	9.24	94.08	1.85	2.74

4.4. Molecular dynamics simulations

Molecular dynamics simulation study was performed to simulate the adsorption structure of the HPD on copper surface in an attempt for understanding the interactions between HPD and copper surface. Molecular structure of HPD shows that it is likely to adsorb on copper surface by sharing the electrons of nitrogen, sulphur and oxygen atoms, phenyl rings and pyrimidine structure with copper. The adsorption progress of HPD on copper surface is investigated by performing molecular mechanics (MM) using MS modeling software. The periodic boundary conditions (PBC) were applied to the simulation cell and described elsewhere [41]. HPD molecule was energy optimized, copper surface was constructed using the amorphous cell module, the whole system was energy optimized and the possibility of HPD adsorption on the copper surface were simulated as in Fig. 5a. It could be seen from Fig. 5a that HPD molecule moves near to the copper surface, indicating that HPD adsorbed at copper surface. Fig. 5a shows that the adsorption occurred through the nitrogen atoms in HPD. During simulation, both in plane aromatic structures are fluctuating up and down the copper surface while nitrogen atoms are attached all the time to copper surface.

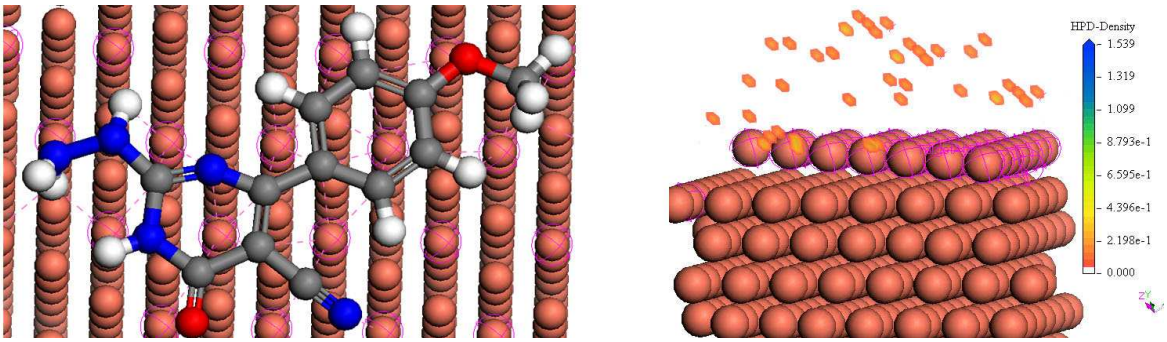

Figure 5 (a) Most suitable configuration for adsorption of HPD on Cu (111) substrate obtained by adsorption locator module, (b) The adsorption density of HPD on the Cu (111) substrate

The adsorption density of HPD on the Cu (111) substrate has been presented in Fig. 5b.Therefore, the studied molecules are likely to adsorb on the copper surface to form a stable adsorption layer and protect copper from corrosion. The binding energies as well as the adsorption energy were calculated and presented in Table 4.

Table 4 Quantum chemical and molecular dynamics parameters derived for HPD calculated with DFT method in aqueous phase

Property	Value
Total energy /kCal mol^{-1}	-78881.8
$E_{\text{Cu-inhibitor}}$ / kcal/mol	-511.7
E_{binding} /kcal/mol	511.7
Adsorption energy/ kcal mol^{-1}	-127.7
Rigid adsorption / energy kcal mol^{-1}	-78.27
Deformation energy/ kcal mol^{-1}	-49.47
dE_{ad}/dN_i kcal mol^{-1}	-127.7

The parameters presented in Table 4 include total energy, in kcal mol^{-1}, of the substrate–adsorbate configuration. The total energy is defined as the sum of the energies of the adsorbate components, the rigid adsorption energy and the deformation energy. In this study, the substrate energy (copper surface) is taken as zero. In addition, adsorption energy in kcal mol^{-1}, reports energy released (or required) when the relaxed adsorbate components (HPD molecule) are adsorbed on the substrate. The adsorption energy is defined as the sum of the rigid adsorption energy and the deformation energy for the adsorbate components. The rigid adsorption energy reports the energy, in kcal mol^{-1}, released (or required) when the unrelaxed adsorbate components (i.e., before the geometry optimization step) are adsorbed on the substrate. The deformation energy reports the energy, in kcal mol^{-1}, released when the adsorbed adsorbate components are relaxed on the substrate surface. Table 6 shows also (dE_{ads}/dNi), which reports the energy, in $kcalmol^{-1}$, of substrate–adsorbate configurations where one of the adsorbate components has been removed. The binding energy introduced in Table 4 calculated from equation (2). The vertical distance, calculated from molecular dynamics, between the flat molecules and copper surface was about 2.9 Å for HPD; this result indicates that the interaction between the HPD molecules and the copper surface is strong enough to inhibit corrosion.

5. Conclusion

The main conclusions of the present study can be summarized as follows:
The electrochemical measurements demonstrated that, under the chosen experimental conditions HPD offers sufficient inhibition against copper corrosion in 3.5% NaCl solutions. Tafel polarization studies have shown that the HPD suppresses both the cathodic and anodic processes and thus it acts as mixed-type inhibitor. The results of EIS indicate that the value of CPEs tends to decrease and both charge transfer resistance and inhibition efficiency tend to increase by increasing the inhibitor concentration. This result can be attributed to increase of the thickness of the electrical double layer. EFM can be used as a rapid and non destructive technique for corrosion rate measurements without prior knowledge of Tafel constants. Molecular dynamic simulations are performed to investigate the adsorption behaviour of HPD on copper surface.

References

1. Sherif, E.M. Park, S.-M. *J. Electrochem. Soc*. 152 (2005) B428.
2. El Warraky, A.A. El Shayeb, H.A. Sherif, E.M. *Anti-Corros. Methods Mater*. 51 (2004) 52;
3. El Warraky, A.A. El Shayeb, H.A. Sherif, E.M. *Egypt. J. Chem.* 47 (2004) 609
4. Hoepner, T. Lattemann, S. *Desalination* 152 (2003) 133.
5. Bacarella, L. Griess, J.C. *J. Electrochem. Soc.* 120 (1973) 459.
6. Qu, J. Guo, X. Chen, Z. *Mater. Chem. Phys.* 93 (2005) 388.
7. Singh, M.M. Rastogi, R.B. Upadhyay, B.N. Yadav, M. *Mater. Chem. Phys.* 80 (2003) 283.
8. Dafali, A., Hammouti, B., Mokhlisse, R., Kertit, S. *Corros. Sci.* 45 (2003) 1619.
9. Lee, H.P. Nobe, K. *J. Electrochem. Soc.* 133 (1986) 2035.
10. C. Wang, Chen, S., Zhao, S. *J. Electrochem. Soc.* 151 (2004) B11.
11. Kendig, M., Jeanjaquet, S. *J. Electrochem. Soc.* 149 (2002) B47.
12. Crousier, J., Pardessus, L., Croussier, J. P. *Electrochim. Acta*, 33 (1988)1039.
13. Bertocci, U., Turner, D., in Encyclopedia of Electrochemistry of the Elements, Vol II, ed, A.J. Bard, Marcel Dekker, New York,1974.
14. Muydler, V. J., in Comprehensive Treatise of Electrochemistry, Vol. 4, ed. J'OM, Bockris, B.E. Conway, E.Yeager, and R.E. White. Plenum Press, New York, 1981, pp. 1-96.
15. Speckmann, H.D., Strehblow, H.H. *Werkst Korros.,* 35 (1984) 512.
16. Cicileo, G. P., Rosales, B. M., Varela, E., Vilche J. R. *Corros. Sci*., 39 (1998)1915.
17. Granese, S.L., Rosales, B.M., Oviedo, C., Zerbino, J.O. *Corros. Sci.*, 33 (1992) 1439.
18. Cicileo, G.P., Rosales, B. M., Vilche, J.R. in Proceeding`s 7th European Symp. Corrosion Inhibitors, Ferrara, Italy, 1995, p. 1011.
19. Mansfeld, F., Wang, Y. in *Corrosion 95 NACE*, Paper, No. 41. 1995
20. McMahon, A.J., Harrop, D. *in Corrosion 95 NACE*, Paper No. 32, 1995
21. Brunoro, G., Trabanelli, G., Zucchi, F., in Proceeding `s of 3th European Symp. Corrosion Inhibitors, Ferrara, Italy, 1975, p.443
22. Raicheva, S.N., Sokolova, E.I., Zlateva, D.S., in Proceeding `s of 4th European Symp. Corrosion Inhibitors, Ferrara, Italy, 1980, p. 755
23. R. M. Saleh, M. A. Abd El-Alim and A. A. Hosary, Corrosion Prevention & Control February (1983) 9. 19.

24. Ram, V.J., Berche, D.A.V., Vlietinck, A.J. *J. Heterocycl. Chem.*, 21, 1307 (1984).
25. Barriga, J., Coto, B., Fernandez, B. *Tribol Int.* 40 (2007) 960.
26. Khaled, K.F. *J. Solid Stat Eectrochem.* 13 (2009) 1743.
27. Mineva, T., Parvanov, V., Petrov, I., Neshev, N., Russo, N., *J. Phys. Chem. A* 105 (2001) 1959.
28. Sherif, E.M. *Appl. Surf. Sci.* 252 (2006) 8615.
29. Basics of corrosion measurements, Application note n°.1, (EG&G Prinston Applied Research) p.1.
30. McCafferty, E. *Corros. Sci.* 47 (2005) 3202.
31. Hack, H.P., Pickering, H.W. *J. Electrochem. Soc.* 138 (1991) 690.
32. Khaled, K.F. *Mater. Chem.Pphys.*, 112 (2008) 104-111.
33. Sherif, E.M. Park, S.-M. *Corros. Sci.* 48 (2006) 4065.
34. Juttner, K., Loranz, W. J., Kending, M.W., Mansfeld, F. *J. Electrochem. Soc.* 135 (1988) 335.
35. Juttner, K., Manadhar, K., Seifer-Kraus, V., Loranz, W. J., Schmidt, D. *Werkst, und Korr.* 37 (1986) 377.
36. Ma, H., Chen, S., Niu, L., Zhao, S., Li, S. Li, D. *J. Appl. Electrochem.* 32 (2002) 65.
37. Pajkossy, T. *J. Electroanal. Chem.* 364 (1994) 111.
38. Khaled, K.F. *Mater. Chem. Phys.* 112 (2008) 290.
39. Bosch, R.W., Hubrecht, J., Bogaerts, W.F., Syrett, B.C., *Corrosion* 57 (2001) 60.
40. Abdel-Rehim, S.S., Khaled, K.F., Abdel-Shafi, N.S. *Electrochim. Acta* 51 (2006) 3267.
41. Khaled, K.F. *Electrochim. Acta* 53 (2008) 3484.